

**INTERNATIONAL JOURNAL OF ADVANCES IN
PHARMACY, BIOLOGY AND CHEMISTRY**

Research Article

**Spectroscopic, thermal analyses and biological
activity evaluation of atenolol complexes with
Cr(III), Sr(II), Cd(II) and U(VI)**

Mohamed S. El-Attar^{1, 2}

¹Department of Chemistry, Faculty of Science, Zagazig University, Zagazig, Egypt,

²Department of Chemistry, Faculty of Science, Jzan University, Saudi Arabia.

ABSTRACT

Solid complexes of atenolol were prepared and characterized by elemental analysis, spectral, thermal (TG & DTG), magnetic susceptibility and conductance measurements. Atenolol coordinated to the metal ions as a deprotonated bidentate ligand via oxygen atom of hydroxyl group and the nitrogen atom of secondary amine. The calculated bond length and force constant, $F(U=O)$, in the uranyl complex are 1.877 Å and 677.42 Nm^{-1} , respectively. Also, the kinetic and thermodynamic parameters for the different thermal degradation steps of the complexes were determined by Coats–Redfern and Horowitz–Metzger methods. The antibacterial activities were also tested against *S. aureus*, *E. coli*, *P. aeruginosa* and *B. subtilis* and antifungal screening was studied against two species *C. albicans* and *A. fumigates*. The antimicrobial activity of the metal complexes exhibit higher activities compared with free ligand.

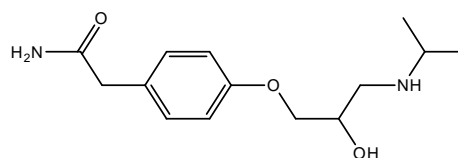
Keywords: Atenolol; ¹H NMR; IR; Thermal analysis and biological activity.

1. INTRODUCTION

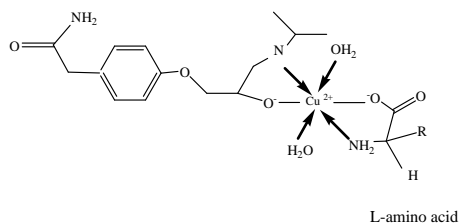
Atenolol, (RS)-2-{4-[2-hydroxy-3-(propan-2-ylamino)propoxy]phenyl} acetamide (Scheme 1) is a drug widely used in blood pressure control as a β -blocker and is used to treat hypertension, sinus tachycardia, arrhythmias, coronary heart disease and myocardial infarction where it acts preferentially upon the adrenergic receptors in the heart ¹⁻⁵. The knowledge of the structure is therefore of utmost importance for understanding the physico-chemical behaviour and biological action of this compound.

Castro et al. ⁶ reported Infrared spectroscopy of racemic and enantiomeric forms of atenolol. The molecular structure of conformational isomorphs given by X-ray diffraction for racemic and enantiomeric atenolol were optimized at the HF/6-31G* level of theory and the infrared spectra of the structure were calculated. These spectra are used to characterize the differences between the various

atenolol conformers. Different approaches of impregnation for resolution of enantiomers of atenolol, propranolol and salbutamol using Cu(II)-l-amino acid complexes for ligand exchange on commercial thin layer chromatographic plates (Scheme 2) were reported ⁷.



Scheme 1. The formula of (RS)-2-{4-[2-Hydroxy-3-(propan-2-ylamino)propoxy]phenyl} acetamide.



Scheme 2. Proposed structure of the ternary complex of atenolol and amino acid with Cu(II).

IR, Raman and surface-enhanced Raman scattering spectra of atenolol and metoprolol were recorded and assigned on the basis of density functional theory (DFT) calculations^{8,9}. The co-ordination mode of the metal ions in Cu(II)-aten and metoprolol compounds was also derived from IR spectra. EPR spectra give evidence for a square-planar arrangement around the copper (II) ion in the case of Cu-aten complex, with a N_2O_2 chromophore.

Our aim was to take synthesize Cr(III), Sr(II), Cd(II) and U(VI) complexes of the atenolol ligand. The structures of the metal complexes were elucidated by elemental analysis, FT-IR, 1H NMR, MS, UV/vis and thermal analysis as well as some results of bioactivity tests are also investigated against *S. aureus*, *E. coli*, *P. aeruginosa* and *B. subtilis* and antifungal screening was studied against two species *C. albicans* and *A. fumigates*.

2. MATERIALS AND METHODS

2.1. Chemicals

All chemicals used for complexes preparation were of analytical reagent grade used without further purification. Atenolol used in this study was purchased from the Egyptian International Pharmaceutical Industrial Company (EIPICO). Ethanol, NaOH and $FeCl_3 \cdot 6H_2O$ were purchased from Fluka Chemical Co. $Cr(CH_3COO)_3$, $CdCl_2$, $SrCl_2$ and $UO_2(CH_3COO)_2 \cdot 2H_2O$ from Aldrich Chemical Co.

2.2. Synthesis of atenolol complexes

The green solid complex $[Cr(Aten)_2(H_2O)_2]CH_3COO \cdot 2H_2O$ was prepared by adding 0.229 g of chromium acetate (1 mmol) in 20 mL ethanol drop-wisely to a stirred mixture of 0.533 g of atenolol (2 mmol) and 0.08 g NaOH (2 mmol) in 50 mL ethanol with molar ratio 1:2 [M]:[Aten]. The reaction mixture was stirred for 20 h at 35 °C in water bath. The grey precipitate was filtered off and dried under vacuum over anhydrous $CaCl_2$.

The white and yellow solid complexes of $[Sr(Aten)_2(H_2O)_2]$, $[Cd(Aten)_2(H_2O)_2] \cdot H_2O$ and

$[UO_2(Aten)_2] \cdot 3H_2O$ were prepared in a similar manner described above using ethanol as a solvent and $SrCl_2$, $CdCl_2$ and $UO_2(CH_3COO)_2 \cdot 2H_2O$, respectively.

2.3. Instruments

Elemental C, H and N analysis was carried out on a Perkin Elmer CHN 2400. The percentage of the metal ions were determined gravimetrically by transforming the solid products into metal oxide and also determined by using atomic absorption method. Spectrometer model PYEUNICAM SP 1900 fitted with the corresponding lamp was used for this purposed. IR spectra were recorded on FTIR 460 PLUS (KBr discs) in the range from 4000 to 400 cm^{-1} . 1H NMR spectra were recorded on Varian Mercury VX-300 NMR Spectrometer using $DMSO-d_6$ as solvent. TG-DTG measurements were run under N_2 atmosphere within the temperature range from room temperature to 1000 °C using TGA-50H Shimadzu; the mass of sample was accurately weighted out in an aluminium crucible. Electronic spectra were obtained using UV-3101PC Shimadzu. The diffused reflectance spectra were recorded on GCMS-QP-1000EX Shimadzu (ESI, 70 eV) in the range from 0-1090. Magnetic measurements were done on a Sherwood scientific magnetic balance using Gouy method using $Hg[Co(SCN)_4]$ as calibrant. Molar conductivities of the solutions of the ligand and metal complexes in DMF at 1×10^{-3} M were measured on CONSORT K410. All measurements were carried out at ambient temperature with freshly prepared solutions.

2.4. Antimicrobial investigation

The activity index for the complex was calculated using the following formula¹⁰:

$$\text{Activity index} = \frac{\text{Zone of inhibition by test compound (diameter)}}{\text{Zone of inhibition by standard (diameter)}}$$

Antimicrobial activity of the ligand and its metal complexes was investigated by a previously reported modified method of Beecher and Wong¹¹ against different bacterial species, such as *S. aureus*, *B. subtilis*, *E. coli*, and *P. aeruginosa* and antifungal screening was studied against two species, *C. albicans* and *A. fumigates*. The tested microorganisms isolates were isolated from Egyptian soil and identified according to the standard mycological and bacteriological keys for identification of fungi and bacteria as stock cultures in the microbiology laboratory, Faculty of Science, Zagazig University. The nutrient nutrient agar medium for antibacterial was 0.5% peptone, 0.1% beef extract, 0.2% yeast extract, 0.5% NaCl and 1.5% agar-agar and for antifungal 3% Sucrose, 0.3%

NaNO₃, 0.1% K₂HPO₄, 0.05% KCl, 0.001% FeSO₄, 2% agar-agar was prepared¹² and then cooled to 47 °C and seeded with tested microorganisms. Sterile water agar layer was poured and solidified. The prepared growth medium for bacteria and fungi (plate of 12 cm diameter, 15 cm³ medium plate). After solidification 5 mm diameter holes were punched by a sterile cork-borer. The investigated compounds, i.e., ligand and their complexes were introduced in Petri-dishes (only 0.1 mL) after dissolving in DMF at 1.0×10⁻³ M. These culture plates were then incubated at 37 °C for 20 h for bacteria and for seven days at 30 °C for fungi. The activity was determined by measuring the diameter of the inhibition zone (in mm). Bacterial growth inhibition was calculated with reference to the positive control, i.e., ampicillin, amoxycillin and cefaloxin.

3. RESULTS AND DISCUSSION

Atenolol reacts with Cr(III), Sr(II), Cd(II) and U(VI) in ethanol at room temperature to form solid complexes. The four complexes were obtained as colored powdered materials and characterized using melting point, magnetic measurements, molar conductance, infrared, electronic, proton nuclear magnetic resonance, mass spectra and thermogravimetric analyses. The molar ratio for all prepared complexes is M:L = 1:2 which was established from the results of the chemical analyses and also all the prepared complexes contain two bound water molecules inside the coordination sphere except in U(VI) complex contains three water molecules outside the coordination sphere. The elemental analysis was in good agreement with the chemical formulas of all synthesized complexes. The infrared spectroscopic and thermogravimetric data also confirm the presence of water in the complexes composition. The solution of Cr(III) complex was tested with aqueous solution of FeCl₃.6H₂O a red brown color which revealed the presence of CH₃COO⁻ as counter ion¹³.

The molar conductance values of the atenolol and their metal complexes in DMF with standard reference, using 1×10⁻³ M solutions at room temperature were found to be in the range from 27.4 to 144.8 S cm² mol⁻¹. The data indicated that all complexes are non-electrolyte except Cr(III) complex is electrolyte due to the acetate ion found as counter ion (Table 1). The Sr(II), Cd(II) and U(VI) complexes were found in diamagnetic character with molecular geometries octahedral but the Cr(III) complex found in paramagnetism with measured magnetic moment value at 3.81 B.M.

3.1. IR absorption spectra

The observed frequencies in the IR spectra of free atenolol and its complexes, their relative intensities, and assignments are given in Fig. 1 and Table 2. The IR spectra of the complexes are compared with those of the free ligand in order to determine the coordination sites that may be involved in chelation. The infrared spectra of atenolol metal complexes exhibit a broad band between 3460 and 3352 cm⁻¹, which corresponds to the (O-H) vibration and confirms the presence of water molecules in all complexes¹⁴⁻¹⁶. The (N-H) of -NH and -NH₂ vibration appears in the region of 3300-3171 cm⁻¹¹⁷. The stretching vibrations (C-H) of phenyl, CH₂ and CH₃ units in these complexes are assigned as a number of bands in the region of 3060-2866 cm⁻¹. The assignments of all the C H stretching vibrations agree quite well with the expected in the literature¹⁸⁻²⁰.

Experimentally, The IR band observed at 1643 cm⁻¹ in the spectrum of the free atenolol is characteristic to the stretching vibration of carbonyl group (C=O)²¹. The appearance of this band in all complexes at around 1643 cm⁻¹ indicated that the carbonyl group is uncoordinated to the metal ion.

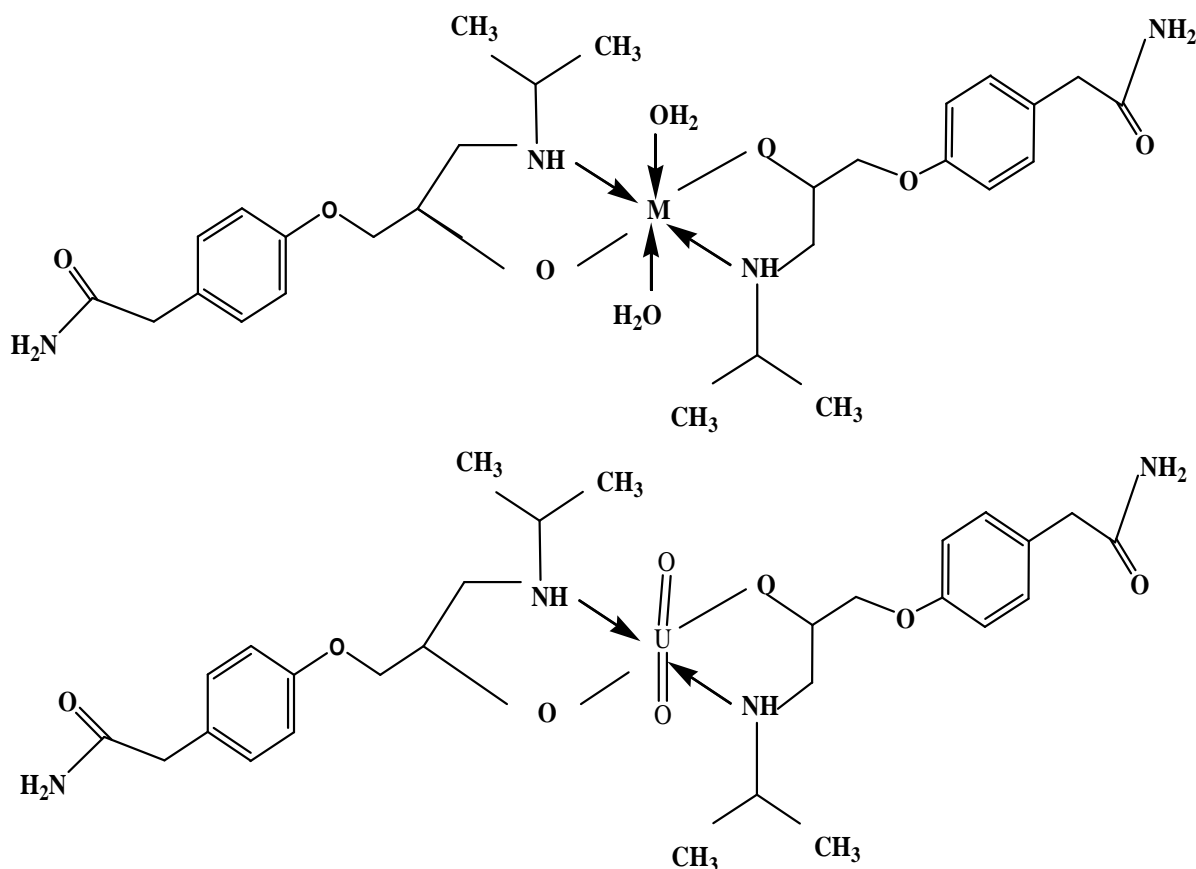
The spectra of the isolated solid complexes show a group of bands with different intensities which characteristics for (M-N),(M-O). The (M-N) and (M-O) bands observed at 630, 529 and 420 cm⁻¹ for Cr(III), at 579 and 459cm⁻¹ for Sr(II), at 671 and 428 cm⁻¹ for Cd(II) and finally at 680, 644, 575 and 443 cm⁻¹ for U(VI) which are absent in the spectrum of atenolol. This indicates the coordination of atenolol through both N-H and oxygen of hydroxyl group.

For [Cr(Aten)₂(H₂O)₂]CH₃COO.2.5H₂O complex in order to verify that the acetate group is ionic and not coordinated, the complex solution was tested with an aqueous solution of FeCl₃.6H₂O a red brown color was formed. Also, characteristic bands of acetate ion are found at 1416, 1360 and 648 cm⁻¹ which assigned to the methyl bending vibrations.

For [UO₂(Aten)₂].3H₂O complex, the proposed structure is shown in scheme 3, where the two oxygen atoms and two nitrogen atoms of their Aten occupy equatorial positions around the central U(VI), forming a plane containing the five membered rings and the two oxygen atoms of the uranyl group occupy axial positions. According to the proposed structure for the uranyl complex, the complex possess a plane of symmetry and hence is C_s symmetry. The C_s group is expected to display 243 vibrational fundamentals which are all monodegenerate. These are distributed between A¹ and A¹ motions, all are IR and Raman active. Under such symmetry, the four vibrations of the uranyl unit, UO₂, in the complex are of the type 3 A¹ and A¹, these are _s(U=O), A¹; _{as}(U=O), A¹;

(UO₂), A^I and (UO₂), A^{II}. The data given in table 2 showed that $\nu_{as}(U=O)$ absorption band occurs as a medium singlet at 926 cm⁻¹ and the $\nu_s(U=O)$ found at 856 cm⁻¹ as a strong band. These assignments for the stretching vibrations of the uranyl group, UO₂, agree quite well with those known for many dioxouranium

(VI) complexes^{17, 21-25}. The $\nu_s(U=O)$ value was used to calculate both the bond length and the bond stretching force constant, F(U=O), for UO₂ bond in our complex^{22, 24}. The calculated bond length and force constant values are 1.877 Å and 677.42 Nm⁻¹, respectively.



M = Cr(III), Sr(II) and Cd(II)

Scheme 3.

The coordination mode of M and U(VI) with atenolol

3.2. Electronic spectra

Experimentally, the electronic reflection spectra of atenolol and the solid complexes were recorded from 200 to 800 nm as shown in Fig. 2 and Table 3. The reflection spectrum of free atenolol displays two bands at 300 and 368 nm. The electronic transition at

300 nm is assigned to higher energy $n \rightarrow \pi^*$ transition within the phenyl ring of the atenolol and the lower energy $n \rightarrow \pi^*$ transition found at 368 nm these transitions occur in case of organic compounds which contain phenyl and keto groups^{26, 27}. For the our complexes, the reflectance bands shift of atenolol to

higher or lower values and the absent of the band at 300 nm and presence of new bands in the reflection spectra of complexes is attributed to complexation behavior of atenolol towards metal ions²⁶. The four complexes have new bands in the range from 490 to 593 nm which may be assigned to the ligand to metal charge-transfer²⁸⁻³⁰. Finally, the metal ions form stable solid complexes with atenolol ligand.

3.3. ¹H NMR spectra

The ¹H NMR spectral data of atenolol and Cr(III), Sr(II), Cd(II) and U(VI) complexes in DMSO-d₆ were measured (Fig. 3). ¹H NMR spectral data (Table 4) indicated the coordination of atenolol with metal ions via N atom (-NH group) and oxygen ion of hydroxyl group. The ¹H NMR spectra of atenolol showed at δ : 0.97 and 1.50 ppm corresponding to -CH₃ and -NH, respectively. A series of bands found in the range 2.54-3.91 ppm are assigned to -CH₂ and -CH aliphatic. Also the ¹H NMR spectra for complexes exhibit new peak in the range 4.87-5.11 ppm, due to the presence of water molecules in the complexes. Atenolol show peaks in the range δ : 6.85-7.41 ppm for the protons of aromatic ring, -NH₂ and the singlet peak at δ : 5.00 ppm for the proton of hydroxyl group. Comparing the main signals of the complexes with atenolol, the ¹H NMR spectra of the complexes show chemical shift values that were only slightly changed compared with the free ligand, except for the hydroxyl proton signal, the resonance of the hydroxyl proton (OH) was not detected in the spectra of the four complexes, suggesting coordination of atenolol through its oxygen of hydroxyl group³¹.

3.4. Mass spectra

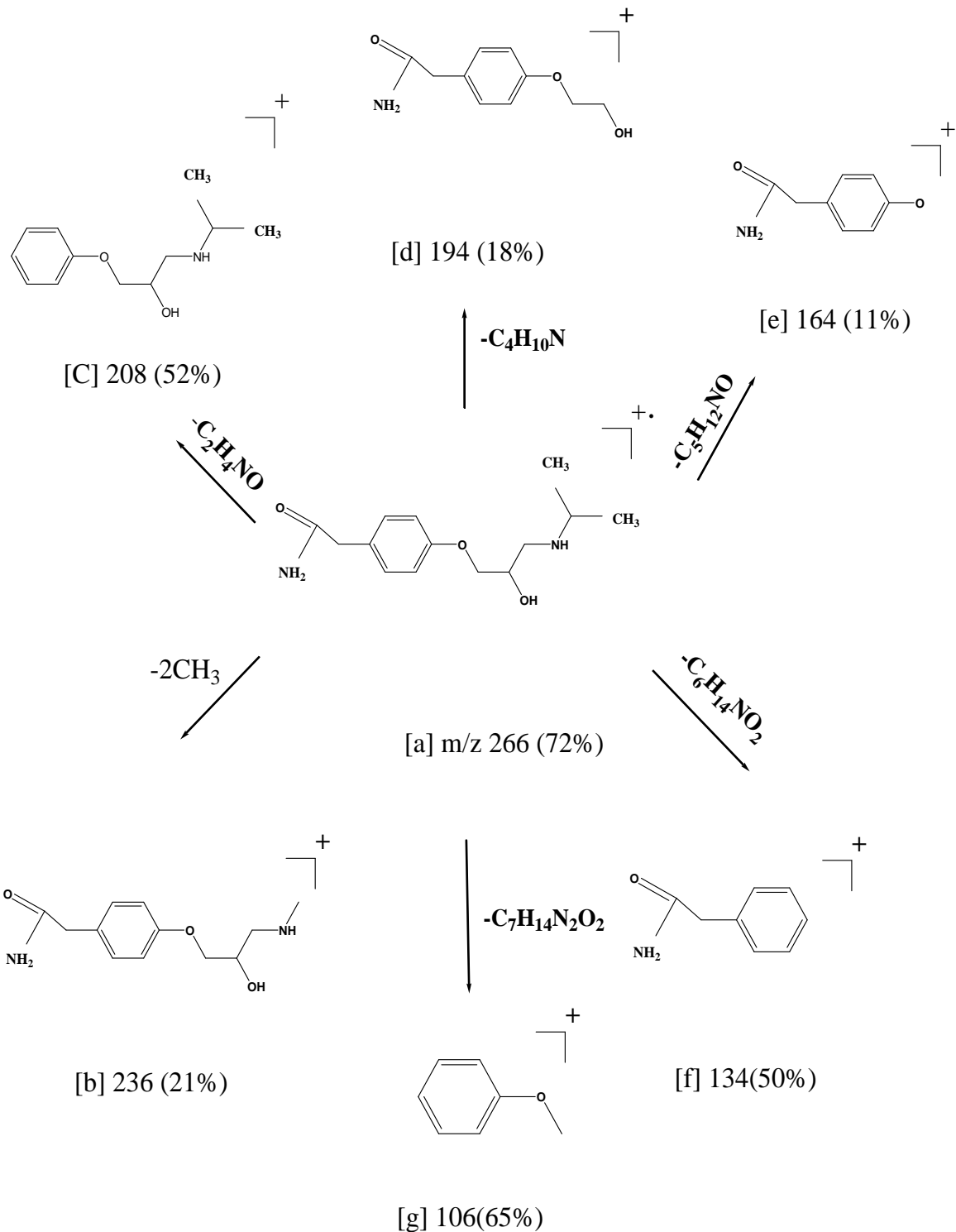
Mass spectrometry was found useful as a complementary tool. The structure and stability of coordination complexes under ionization conditions are dependent on various factors like the ligand itself, metal ion, counter ions, solvent, temperature, concentration,...etc. Mass spectrum of the atenolol (Aten) is in a good agreement with the suggested structure (Fig. 4, Scheme 4). The atenolol showed molecular ion peak (M⁺) at m/z=266 (72%). The molecular ion peak [a] losses C₂H₆ to give fragment [b] at m/z=236 (21%), also it losses C₂H₄NO to give fragment [c] at m/z=208 (52%). The molecular ion peak [a] losses C₄H₁₀N to give fragment [d] at m/z=194 (18%) and it also losses C₅H₁₂NO to give fragment [e] at m/z=164 (11%). It losses C₆H₁₄O₂N to give [f] at m/z=134 (50%) and losses C₇H₁₄N₂O₂ to give fragment [g] at m/z=106 (65%). The mass

spectra of Cr(III), Sr(II), Cd(II) and U(VI) displayed molecular peak at m/z =722 (31%), 654 (29%), 697 (14%) and 863 (60%), respectively, suggesting that the molecular weights of the assigned products matching with elemental and thermogravimetric analyses. Fragmentation pattern of the complex [Cr(Aten)₂(H₂O)₂]CH₃COO.2.5H₂O is given as an example in Scheme 5. The molecular ion peak [a] appeared at m/z=722 (31%) losses C₂H₆ to give [b] at m/z=692 (13%) and it losses C₄H₁₂ to give [c] at m/z=662 (16%). The molecular ion peak [a] losses C₂H₄NO to give [d] at m/z=664 (24%) and it losses C₄H₈N₂O₂ to give [e] at m/z=706 (33%). The molecular ion peak [a] losses C₈H₈NO₂ to give fragment [f] at m/z=572 (12%) and it losses C₁₆H₁₆N₂O₄ to give [g] at m/z=422 (20%).

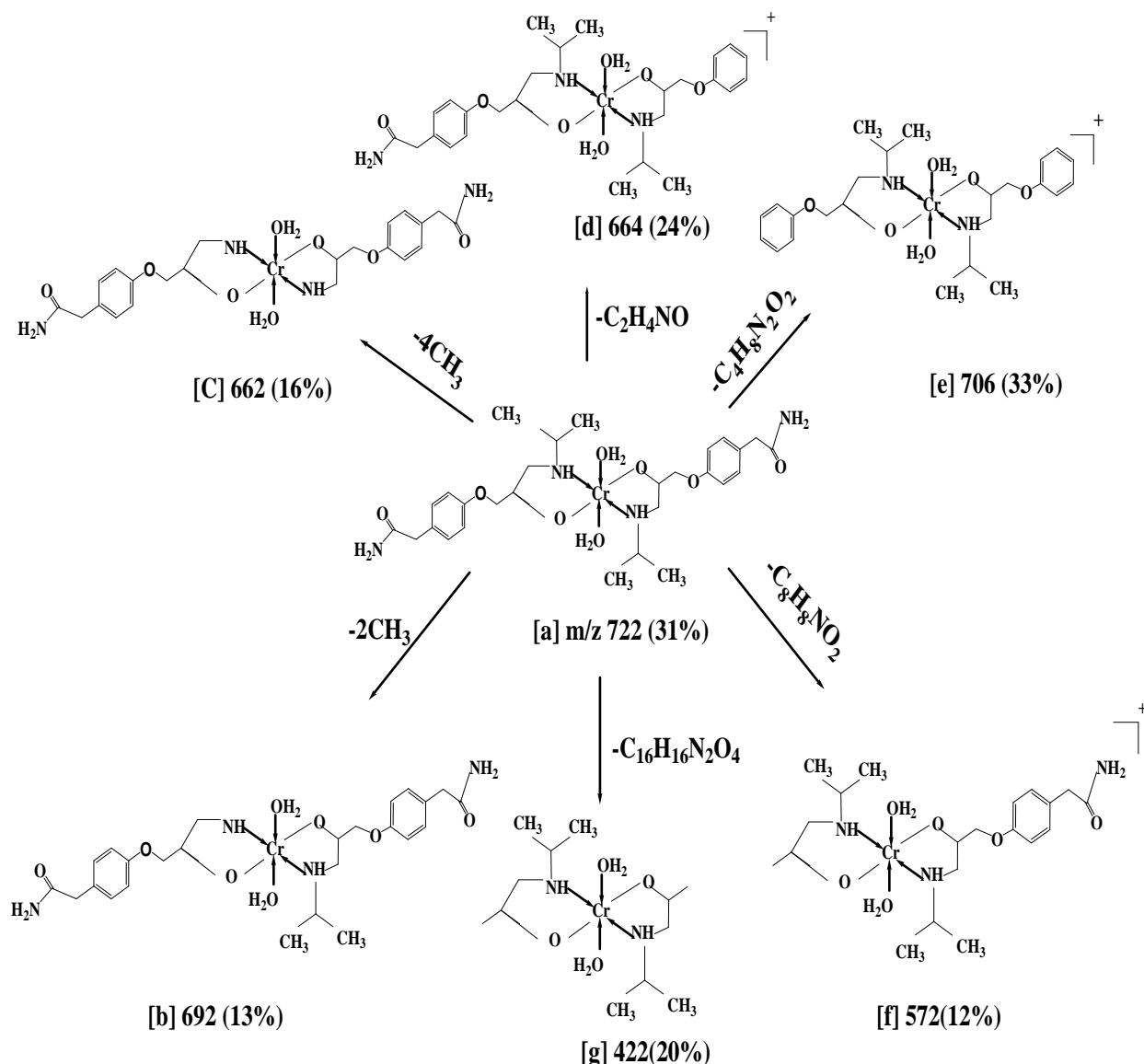
3.5. Thermal studies

The atenolol (Aten) of Cr(III), Sr(II), Cd(II), and U(VI) complexes are stable at room temperature and can be stored for several months without any changes. To establish the proposed formulas for new complexes, thermogravimetric (TG) and differential thermogravimetric (DTG) analyses were carried out for solid complexes under N₂ flow from ambient temperature to 1000 °C. Thermal analysis curves are shown in Fig. 5. Table 5 gives the maximum temperature values, T_{max}/°C together with the corresponding weight loss for each step of the decomposition reactions of the above complexes. The obtained data strongly support the proposed chemical formulas of the complexes under investigation. The data obtained indicated that the atenolol is thermally stable at room temperature. Decomposition of atenolol start at 25 °C and finished at 530 °C with one stage at three maxima 290, 360, and 495 °C and is accompanied by a weight loss of 72.75% corresponding to lose of 4C₂H₄+N₂+3H₂O+6C.

The TG curve of [Cr(Aten)₂(H₂O)₂]CH₃COO.2.5H₂O shows two stages of decomposition. The first stage occurs at maximum temperature 50 °C, 125 °C corresponds to the loss of two and half water molecules with mass loss of 6.21% (calc 6.23%). The second step of decomposition occurs at three maxima at 300, 680 and 960 °C, is accompanied by a weight loss of 75%. This step is associated with the loss of coordinated water molecules and atenolol with intermediate formation of very unstable products which were not identified³²⁻³⁴ forming chromium oxide, CrO_{1.5}+5C, as a final solid product. The actual weight loss from this stage is very close to calculated (74.86%).



Scheme 4.
Fragmentation pattern of free atenolol.



Scheme 5.

Fragmentation pattern of $[\text{Cr}(\text{Aten})_2(\text{H}_2\text{O})_2]\text{CH}_3\text{COO}_2 \cdot 5\text{H}_2\text{O}$.

The $[\text{Sr}(\text{Aten})_2(\text{H}_2\text{O})_2]$ complex decomposes in one step within the temperature range 260-875 °C with total mass loss 76.72% leaving $\text{SrO}+4\text{C}$ as residue.

The thermal decomposition of $[\text{Cd}(\text{Aten})_2(\text{H}_2\text{O})_2] \cdot \text{H}_2\text{O}$ complex in inert atmosphere proceeds approximately with two main degradation steps. The first step of decomposition occurs at maximum temperature of 108 °C and is accompanied by a weight loss of 2.31%, corresponding to the loss of water of crystallization. The second stage of decomposition occurs at maxima temperatures of 275, 460 and 920 °C. The weight loss at this step is 74.12%, corresponding to the loss of $11\text{C}_2\text{H}_4+4\text{NO}+\text{H}_2+3\text{CO}$ as will be described by the

mechanism of the decomposition, the final thermal product obtained is $\text{CdO}+3\text{C}$.

For U(VI) complex the thermal decomposition exhibits two main degradation steps. The first step of decomposition occurs from 67 to 119 °C is accompanied by a weight loss of 6.25% in agreement with the theoretical value 6.32% for the loss of three uncoordinated water molecules. The second step of decomposition occurs at three maxima 229, 286 and 556 °C with a weight loss of 59.30% this associated with the loss of atenolol forming uranium oxide as a final product.

3.6. Activation Thermodynamic Parameters

Coats–Redfern³⁵ and Horowitz-Metzger³⁶ are the two methods mentioned in the literature related to kinetic thermodynamic studies; this methods are applied in this study. From the TG curves, the activation energy, E , pre-exponential factor, A , entropy, S^* , enthalpy, H^* , and Gibbs free energy, G^* were calculated by well-known methods; where $S^* = R \ln(Ah/k_B T_s)$, $H^* = E^* - RT$ and $G^* = H^* - T S^*$. The linearization curves of the Coats–Redfern method is shown in Fig. 6. Kinetic parameters are calculated by employing the Coats–Redfern and Horowitz-Metzger equations, and are summarized in Table 6.

Coats–Redfern equations

$$\ln X = \ln \left[\frac{-\ln(1-X)^{1-n}}{T^2(1-n)} \right] \cong \frac{-E^*}{RT} + \ln \left[\frac{AR}{qE^*} \right] \text{ for } n \neq 1 \quad (1)$$

where ($n = 0, 0.33, 0.5$ and 0.66)

$$\ln X = \ln \left[\frac{-\ln(1-X)}{T^2} \right] \cong \frac{-E^*}{RT} + \ln \left[\frac{AR}{qE^*} \right] \text{ for } n=1 \quad (2)$$

Horowitz-Metzger equations

$$\ln X = \ln \left[\frac{-\ln(1-X)^{1-n}}{T^2(1-n)} \right] \cong \frac{-E^*}{RT} + \ln \left[\frac{AR}{qE^*} \right] \text{ for } n \neq 1 \quad (3)$$

where ($n = 0, 0.33, 0.5$ and 0.66)

$$\ln X = \ln \left[\frac{-\ln(1-X)}{T^2} \right] \cong \frac{-E^*}{RT} + \ln \left[\frac{AR}{qE^*} \right] \text{ for } n=1 \quad (4)$$

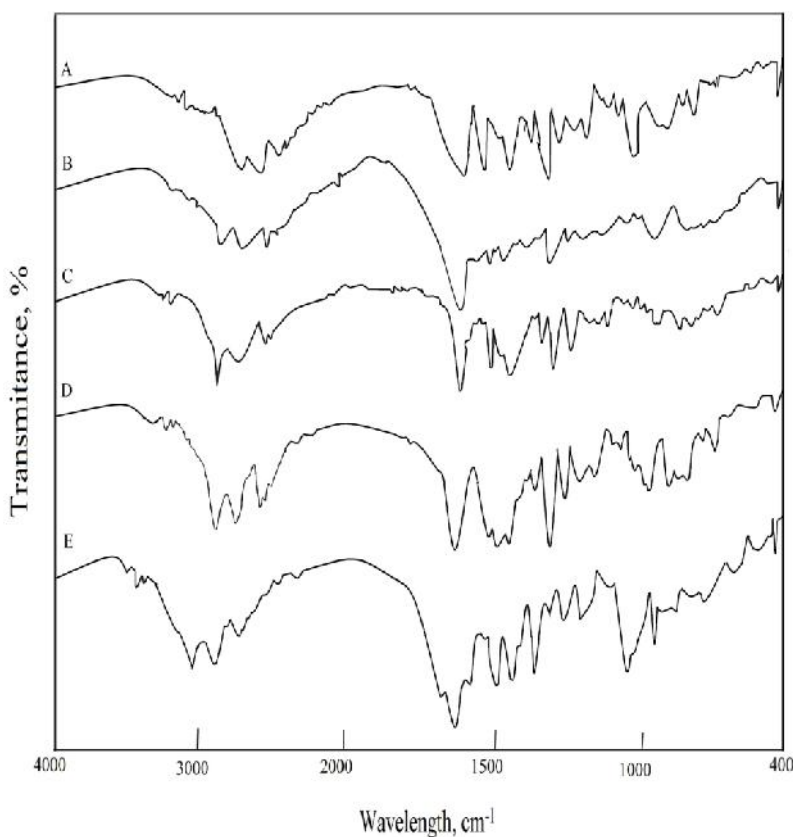


Fig. 1.
Infrared spectra for (A) Atenolol, (B) $[\text{Cr}(\text{Atn})_2(\text{H}_2\text{O})_2](\text{CH}_3\text{COO}) \cdot 2.5\text{H}_2\text{O}$, (C) $[\text{Sr}(\text{Atn})_2(\text{H}_2\text{O})_2]$, (D) $[\text{Cd}(\text{Atn})_2(\text{H}_2\text{O})_2] \cdot \text{H}_2\text{O}$ and (E) $[\text{UO}_2(\text{Atn})_2] \cdot 3\text{H}_2\text{O}$

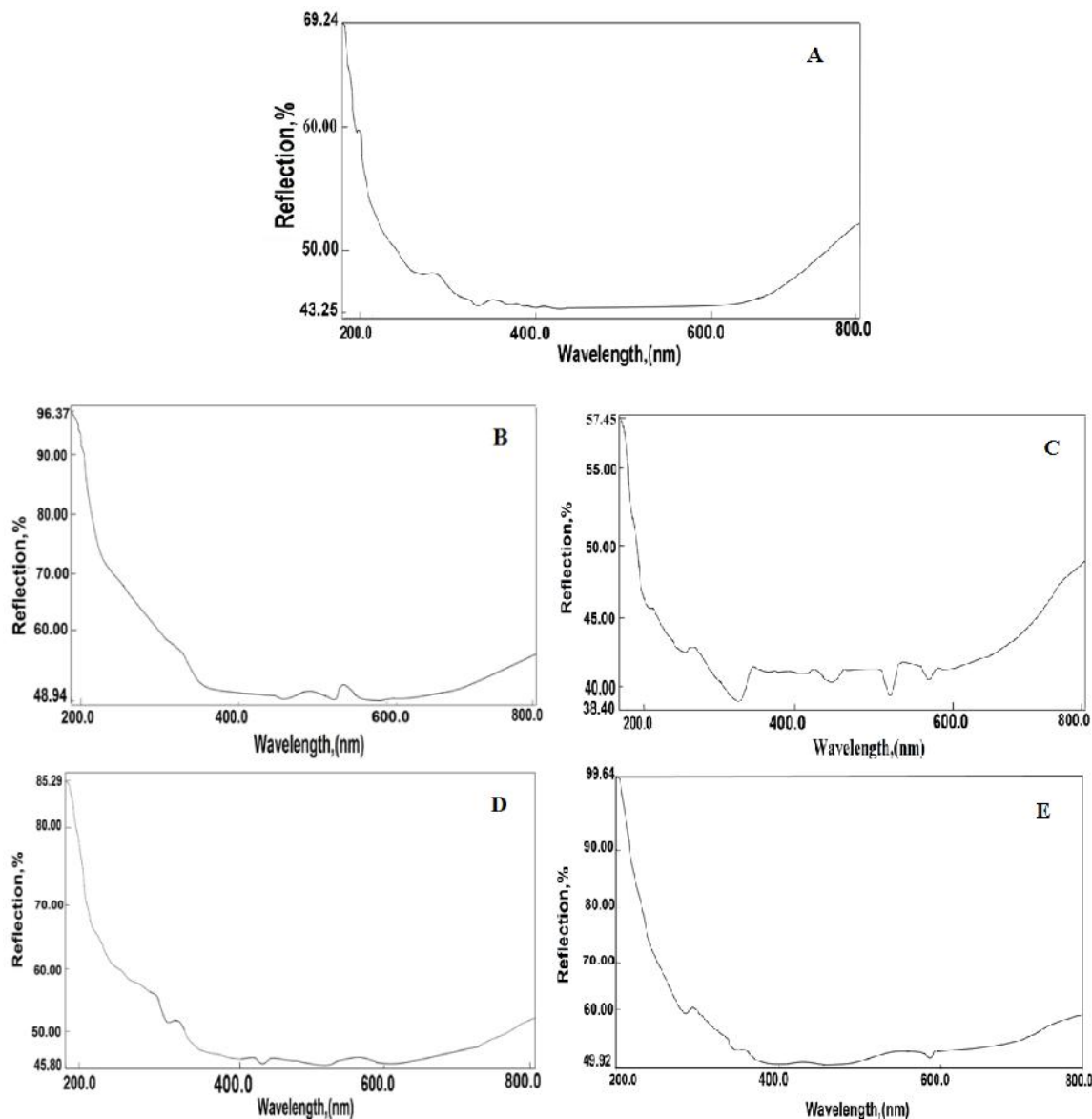


Fig. 2.

Electronic reflection spectra for (A) Atenolol, (B) $\text{Cr}(\text{Aten})_2(\text{H}_2\text{O})_2]\text{CH}_3\text{COO}.2.5\text{H}_2\text{O}$, (C) $[\text{Sr}(\text{Aten})_2(\text{H}_2\text{O})_2]$, (D) $[\text{Cd}(\text{Aten})_2(\text{H}_2\text{O})_2].\text{H}_2\text{O}$ and (E) $[\text{UO}_2(\text{Aten})_2].3\text{H}_2\text{O}$.

The activation energies of decomposition were found to be in the range $61.62\text{--}104.45\text{ kJ mol}^{-1}$. The high values of the activation energies reflect the thermal stability of the complexes^{37, 38}. The entropy of activation was found to have negative values in all the complexes which indicate that the decomposition reactions proceed with a lower rate than the normal ones. Also, the correlation coefficients of Arrhenius plots (R) of the thermal decomposition steps were found to lie in the range $0.995\text{--}0.999$, showing a good fit with linear function.

3.7. Antimicrobial investigation

The susceptibility of certain strains of bacterium, such as *S. aureus*, *E. coli*, *P. aeruginosa* and *B. subtilis* and antifungal screening was studied against two species *C. albicans* and *A. fumigates* towards atenolol and its complexes was judged by measuring size of the inhibition diameter. As assessed by color, the complexes remain intact during biological testing (Table 7 and Fig. 7).

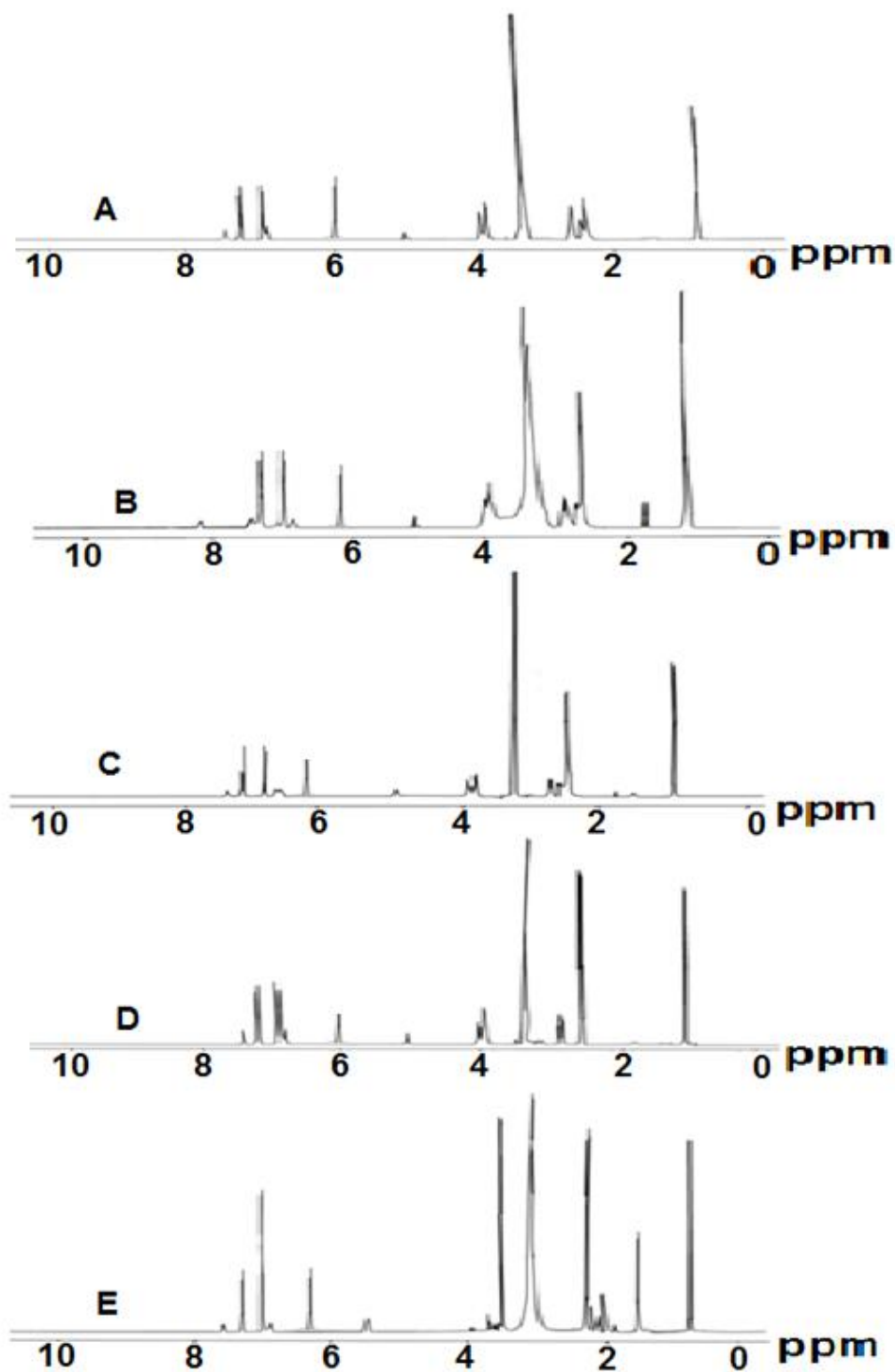


Fig. 3.

^1H NMR spectra for (A) Atenolol; (B) $[\text{Cr}(\text{Aten})_2(\text{H}_2\text{O})_2]\text{CH}_3\text{COO}\cdot 2.5\text{H}_2\text{O}$, (C) $[\text{Sr}(\text{Aten})_2(\text{H}_2\text{O})_2]$, (D) $[\text{Cd}(\text{Aten})_2(\text{H}_2\text{O})_2]\cdot\text{H}_2\text{O}$ and (E) $[\text{UO}_2(\text{Aten})_2]\cdot 3\text{H}_2\text{O}$.

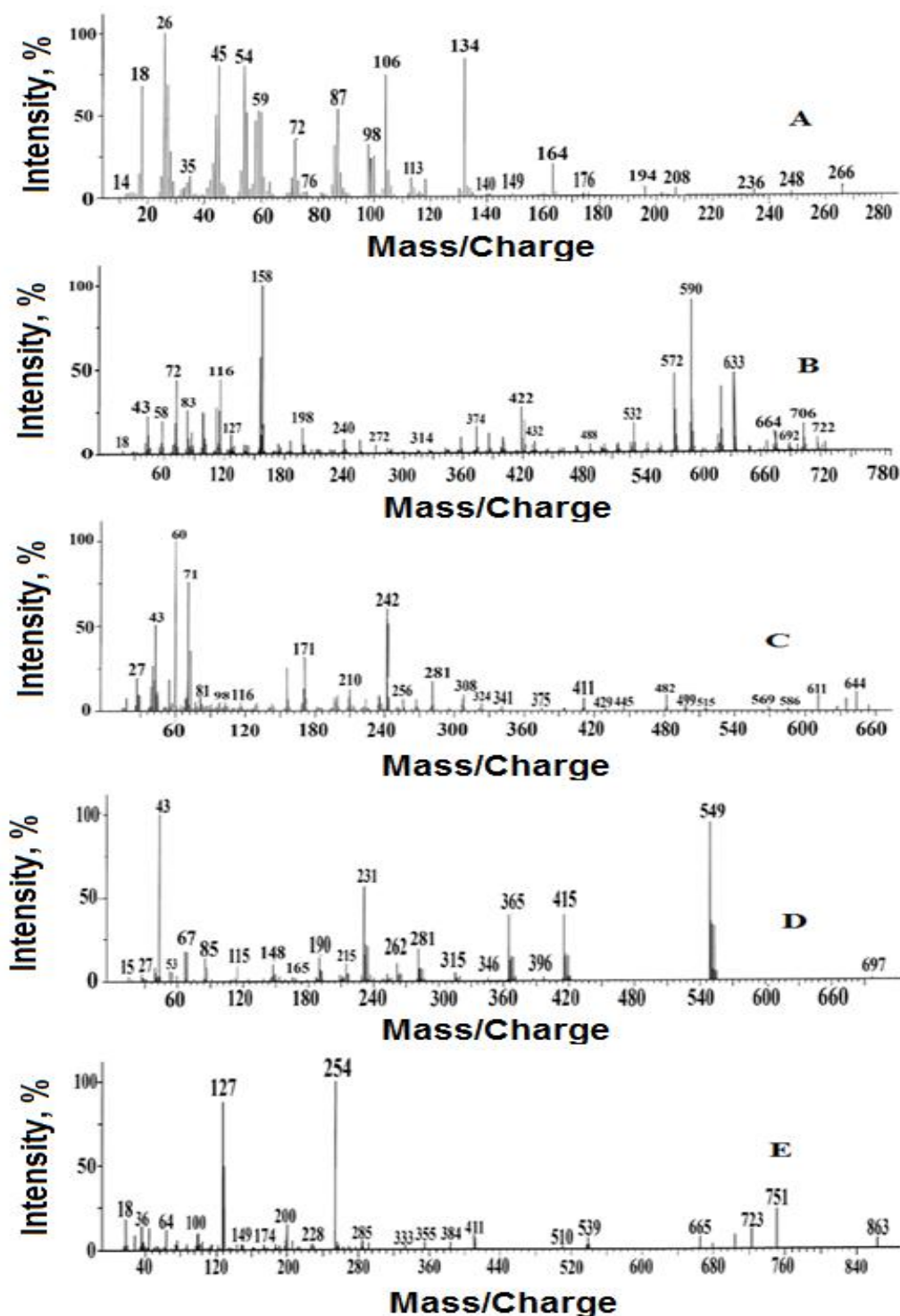


Fig. 4.

Mass spectra of (A) Atenolol; (B) $[\text{Cr}(\text{Aten})_2(\text{H}_2\text{O})_2]\text{CH}_3\text{COO} \cdot 2.5\text{H}_2\text{O}$,
 (C) $[\text{Sr}(\text{Aten})_2(\text{H}_2\text{O})_2]$, (D) $[\text{Cd}(\text{Aten})_2(\text{H}_2\text{O})_2] \cdot \text{H}_2\text{O}$ and (E) $[\text{UO}_2(\text{Aten})_2] \cdot 3\text{H}_2\text{O}$.

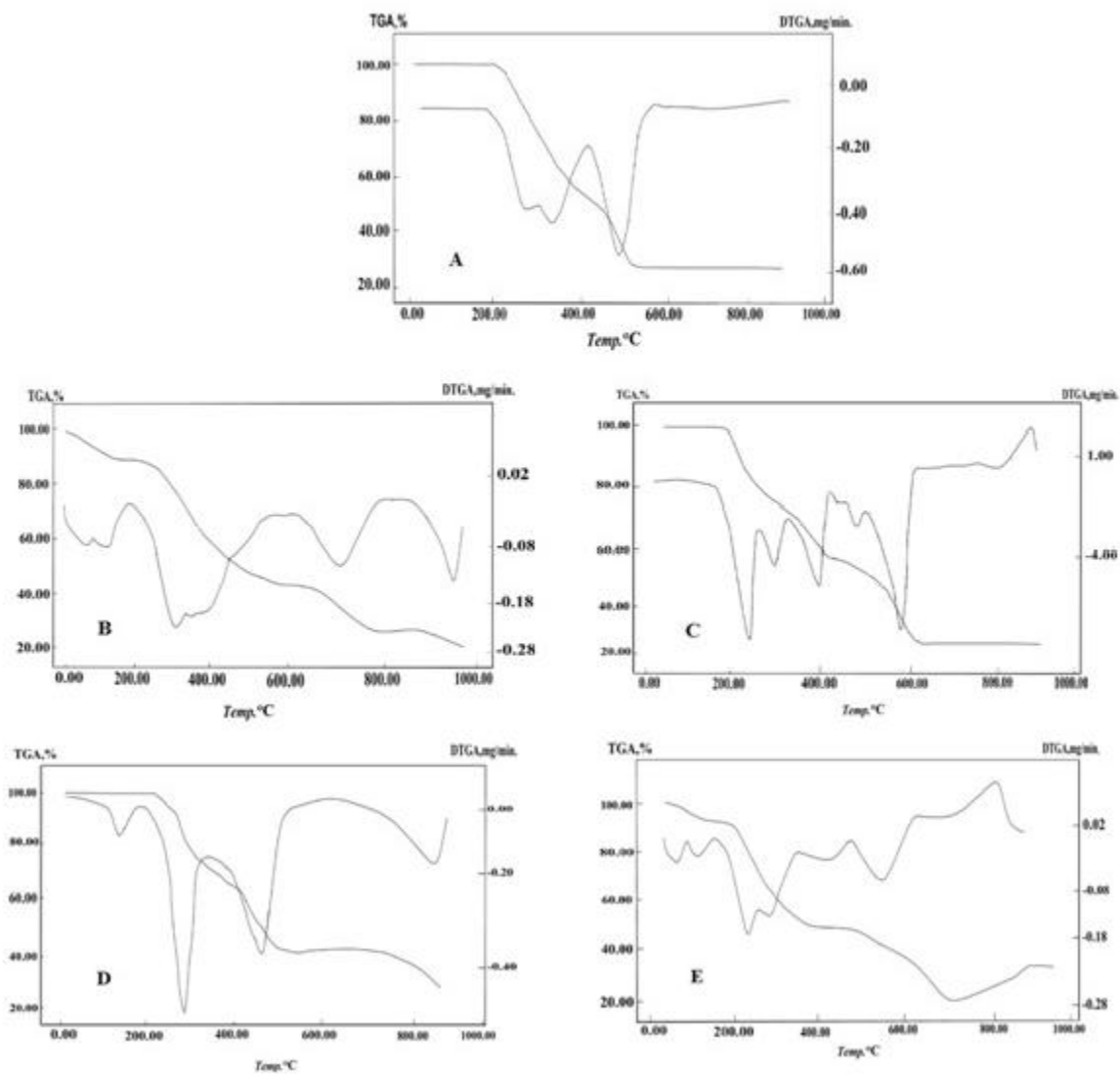
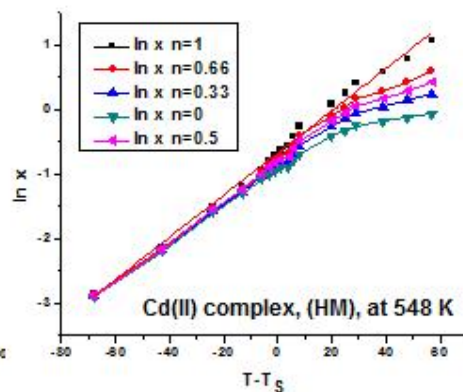
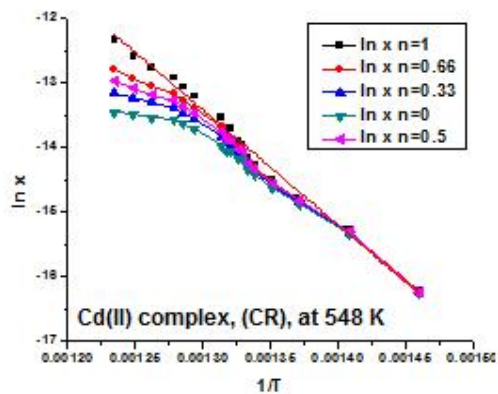
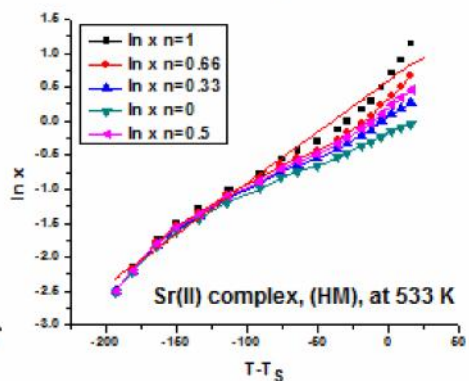
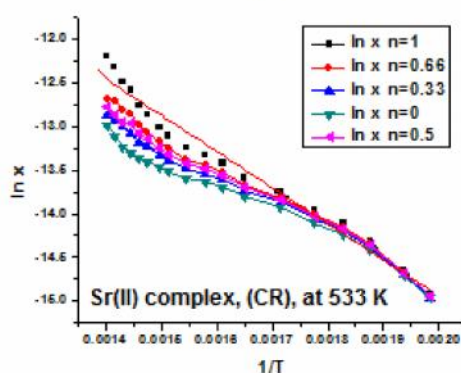
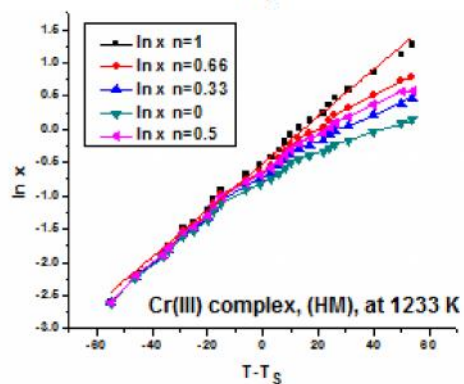
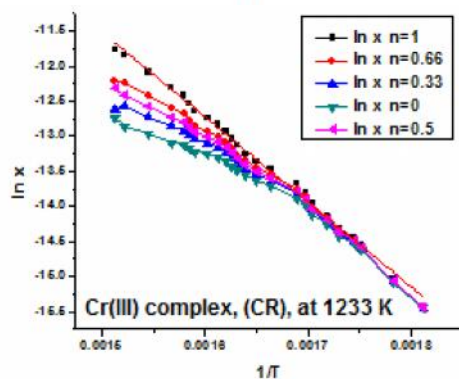
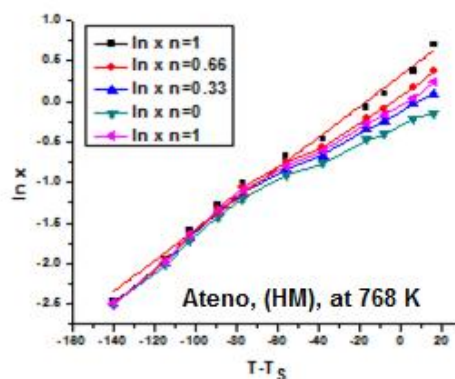
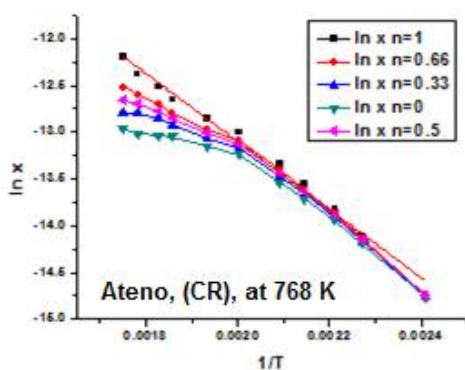


Fig. 5.

TGA and DTG diagram for(A) Atenolol; (B) $[\text{Cr}(\text{Aten})_2(\text{H}_2\text{O})_2]\text{CH}_3\text{COO}.2.5\text{H}_2\text{O}$, (C) $[\text{Sr}(\text{Aten})_2(\text{H}_2\text{O})_2]$, (D) $[\text{Cd}(\text{Aten})_2(\text{H}_2\text{O})_2].\text{H}_2\text{O}$ and (E) $[\text{UO}_2(\text{Aten})_2].3\text{H}_2\text{O}$.



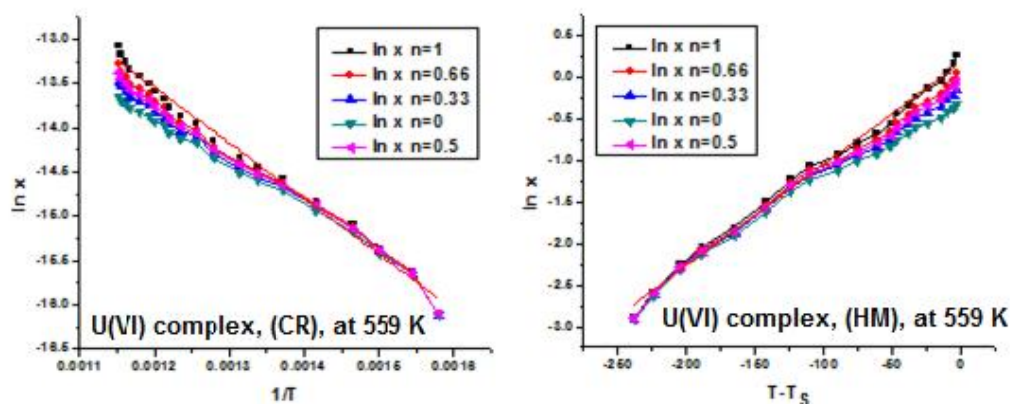


Fig. 6. The diagrams of kinetic parameters of atenolol and its metal complexes using Coats-Redfern (CR) and Horowitz-Metzger (HM) equations.

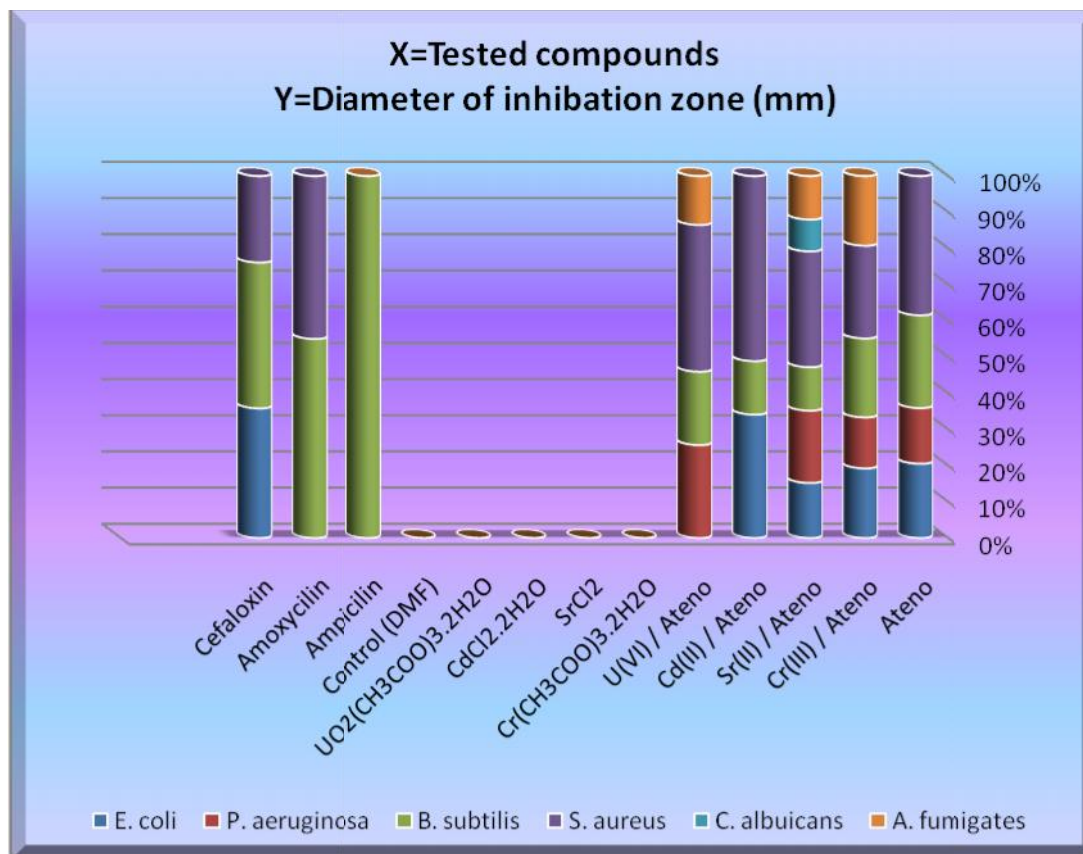


Fig. 7. Statistical representation for biological activity of atenolol and its metal complexes.

Table 1
Elemental analysis and physico-analytical data for atenolol and its metal complexes

Compounds M.Wt. (M.F.)	Yield%	Mp/ C	Color	Found (Calcd.) (%)				μ_{eff} (B.M.)	(S cm ² mol ⁻¹)
				C	H	N	M		
Atenolol (Aten) 266.34 (C ₁₄ H ₂₂ N ₂ O ₃)	-	160	White	63.10 (63.13)	8.30 (8.33)	12.32 (12.38)	-	Diamagnetic	27.4
[Cr(Aten) ₂ (H ₂ O) ₂]CH ₃ COO.2.5H ₂ O 722.77 (CrC ₃₀ H ₅₄ N ₄ O _{12.5})	73.54	270	Green	49.81 (49.85)	7.50 (7.53)	7.70 (7.75)	7.15 (7.19)	3.81	80.2
[Sr(Aten) ₂ (H ₂ O) ₂] 654.31 (SrC ₂₈ H ₄₆ N ₄ O ₈)	77.98	180	White	51.34 (51.39)	7.04 (7.09)	8.52 (8.56)	13.32 (13.39)	Diamagnetic	26.9
[Cd(Aten) ₂ (H ₂ O) ₂].H ₂ O 696.75 (CdC ₂₈ H ₄₈ N ₄ O ₉)	76.42	240	White	48.22 (48.27)	6.90 (6.94)	8.01 (8.04)	16.09 (16.13)	Diamagnetic	28.0
[UO ₂ (Aten) ₂].3H ₂ O 854.70 (UC ₂₈ H ₄₈ N ₄ O ₁₁)	80.52	170	Yellow	39.31 (39.35)	5.61 (5.66)	6.51 (6.56)	27.81 (27.85)	Diamagnetic	29.3

Table 2
Selected infrared absorption frequencies (cm⁻¹) of ligand and its complexes.

Compounds	(O-H); H ₂ O and COOH	(N-H); -NH and -NH ₂	(C=O)	_{as} (U=O) and _s (U=O)	(M-O) and (M-N)
Atenolol	3572w 3355s	3300sh 3171s	1643vs	-	-
[Cr(Aten) ₂ (H ₂ O) ₂]CH ₃ COO.2.5H ₂ O	3460vw 3356ms	3280sh 3175ms	1643s	-	648vw 630vw 529m 420vw
[Sr(Aten) ₂ (H ₂ O) ₂]	3356s	3317s	1643vs	-	660sh 579m 459vw
[Cd(Aten) ₂ (H ₂ O) ₂].H ₂ O	3356vs	3175s	1639vs	-	671w 583m
[UO ₂ (Aten) ₂].3H ₂ O	3352ms	3171ms	1639m	926m 856s	680w 644w 575w 529m 443w

Keys: s=strong, w=weak, v=very, m=medium, =stretching, sh=shoulder

Table 3
UV-Vis. spectra of atenolol and its metal complexes.

Assignments (nm)	Aten	Aten complex with			
		Cr(III)	Sr(II)	Cd(II)	U(VI)
- * transitions	300	282	297	304	278
n- * transitions	368	352, 452, 479	368, 417, 450	380, 422, 458	348
Ligand-metal charge transfer	-	576	521, 576	490, 578	575, 593
d-d transition	-	610	-	-	-

Table 4
¹H NMR values (ppm) and tentative assignments for (A) Atenolol;
(B)[Cr(Aten)₂(H₂O)₂]CH₃COO₃.2.5H₂O, (C) [Sr(Aten)₂(H₂O)₂],
(D) [Cd(Aten)₂(H₂O)₂].H₂O and (E) [UO₂(Aten)₂].3H₂O.

A	B	C	D	E	Assignments
0.97	1.18	1.18	1.22	1.23	H, -CH ₃
1.50	1.30	1.46	1.63	1.73	H, -NH
2.54-3.91	2.50-3.87	2.50-3.92	2.48-3.91	2.35-3.92	H, -CH ₂ and -CH aliphatic
-	4.89	4.87	5.02	5.11	H, H ₂ O
5.00	-	-	-	-	H, -OH
6.85-7.41	6.20-8.30	6.40-7.92	6.10-7.81	6.50-7.78	H, -NH ₂ and -CH aromatic

Table 5
The maximum temperature T_{max}(°C) and weight loss values of the decomposition stages for atenolol, Cr(III), Sr(II), Cd(II) and U(VI) complexes.

Lost species	Compounds	Weight loss (%)		T _{max} (°C)	Decomposition
		Found	Calc.		
Atenolol (C ₂₈ H ₄₄ N ₄ O ₆)	First step Total loss Residue	73.00 73.00 27.00	72.75 72.75 27.25	290, 360, 495	4C ₂ H ₄ +N ₂ +3H ₂ O+6C
[Cr(Aten) ₂ (H ₂ O) ₂]CH ₃ COO.2.5H ₂ O (C ₃₀ H ₄₉ N ₄ O ₁₀ Cr)	First step Second step Total loss Residue	6.23 74.86 81.09 18.91	6.21 75.00 81.21 18.79	50, 125 300, 680, 960	2.5H ₂ O 12C ₂ H ₄ +CO ₂ +2NO+2NO ₂ +0.5H ₂ O CrO _{1.5} +5C
[Sr(Aten) ₂ (H ₂ O) ₂] (C ₂₈ H ₄₆ N ₄ O ₈ Sr)	First step Total loss Residue	76.72 76.72 23.17	76.80 76.80 23.20	260, 355, 490, 573	11C ₂ H ₄ +4NO+2CO+H ₂ O SrO+4C
[Cd(Aten) ₂ (H ₂ O) ₂].H ₂ O (C ₂₈ H ₄₆ N ₄ O ₈ Cd)	First step Second step Total loss Residue	2.58 73.77 76.35 23.65	2.31 74.12 76.43 23.57	108 275, 460, 920	H ₂ O 11C ₂ H ₄ +4NO+H ₂ +3CO CdO+3C
[UO ₂ (Aten) ₂].3H ₂ O (C ₂₈ H ₄₄ N ₄ O ₉ U)	First step Second step Total loss Residue	6.25 59.30 65.55 34.45	6.32 59.28 65.60 34.40	67, 119 229, 286, 556	3H ₂ O 10C ₂ H ₄ +2N ₂ +6CO+H ₂ UO ₂ +2C

Table 6
Thermal behavior and Kinetic parameters determined using Coats–Redfern (CR) and Horowitz–Metzger (HM) operated for atenolol and its complexes.

Compounds	Decomposition Range (K)	T _s (K)	Method	Parameter					R ^a	SD ^b
				E* (KJ/mol)	A (s ⁻¹)	S* (KJ/mol.K)	H* (KJ/mol)	G* (KJ/mol)		
Aten (C ₁₄ H ₂₂ N ₂ O ₃)	693-843	768	CR	68.67	1.27×10 ⁵	-0.1513	64.57	139.17	0.995	0.05
			HM	85.48	8.04×10 ⁶	-0.1169	81.38	139.00	0.995	0.11
[Cr(Aten) ₂ (H ₂ O) ₂]CH ₃ CO O.2.5H ₂ O (CrC ₃₀ H ₅₄ N ₄ O _{12.5})	1173-1273	1233	CR	104.45	4.12×10 ⁹	-0.0648	100.46	131.58	0.997	0.064
			HM	120.99	1.55×10 ¹¹	-0.0347	116.99	133.64	0.997	0.072
[Sr(Aten) ₂ (H ₂ O) ₂] (SrC ₂₈ H ₄₆ N ₄ O ₈)	473-584	533	CR	91.83	3.65×10 ⁶	-0.1241	87.39	153.67	0.999	0.03
			HM	97.87	2.58×10 ⁷	-0.1079	93.43	151.03	0.999	0.03
[Cd(Aten) ₂ (H ₂ O) ₂].H ₂ O (CdC ₂₈ H ₄₈ N ₄ O ₉)	493-653	548	CR	68.08	5.04×10 ³	-0.1792	63.48	162.56	0.995	0.090
			HM	73.91	4.64×10 ⁴	-0.1607	69.31	158.18	0.995	0.114
[UO ₂ (Aten) ₂].3H ₂ O (UC ₂₈ H ₄₈ N ₄ O ₁₁)	443-660	559	CR	61.62	4.71×10 ³	-0.1793	57.26	151.39	0.995	0.085
			HM	74.20	1.30×10 ⁵	-0.1517	69.84	149.47	0.996	0.084

a=correlation coefficients of the Arrhenius plots and b=standard deviation

Table 7
The inhibition diameter zone values (mm) for atenolol and its metal complexes.

Tested compounds	Microbial species					
	Bacteria				Fungi	
	<i>E. coli</i>	<i>P. aeruginosa</i>	<i>B. subtilis</i>	<i>S. aureus</i>	<i>C. albicans</i>	<i>A. fumigates</i>
Aten	-	6 ± 0.12	10 ± 0.1	15 ± 0.11	-	-
Cr(III) / Aten	15 ⁺² ± 0.01	11 ⁺¹ ± 0.14	17 ⁺¹ ± 0.11	20 ⁺¹ ± 0.18	-	15 ⁺² ± 0.08
Sr(II) / Aten	19 ⁺² ± 0.02	25 ⁺² ± 0.03	15 ⁺¹ ± 0.12	40 ⁺³ ± 0.53	11 ⁺¹ ± 0.30	15 ⁺² ± 0.09
Cd(II) / Aten	30 ⁺³ ± 0.33	-	13 ^{NS} ± 0.10	45 ⁺³ ± 0.55	-	-
U(VI) / Aten	-	19 ⁺² ± 0.02	15 ⁺¹ ± 0.13	30 ⁺² ± 0.08	-	10 ⁺¹ ± 0.06
Cr(CH ₃ COO) ₃ .2H ₂ O	-	-	-	-	-	-
SrCl ₂	-	-	-	-	-	-
CdCl ₂ .2H ₂ O	-	-	-	-	-	-
UO ₂ (CH ₃ COO) ₃ .2H ₂ O	-	-	-	-	-	-
Control (DMF)	-	-	-	-	-	-
Standard	Ampicilin	-	-	28 ± 0.40	-	-
	Amoxycilin	-	-	22 ± 0.11	18 ± 1.73	-
	Cefaloxin	24 ± 0.34	-	27 ± 1.15	16 ± 0.52	-

Statistical significance P^{NS} P not significant, P > 0.05; P⁺¹ P significant, P < 0.05; P⁺² P highly significant, P < 0.01; P⁺³ P very highly significant, P < 0.001; student's, *t*-test (Paired).

A comparative study of ligand and its metal complexes showed that the Cr(III) complex showed highly significant against *E. coli* and significant difference for the other three types of bacteria and highly significant against *A. fumigates* than free ligand. The Sr(II) complex showed very highly significant for *S. aureus* and highly significant against *E. coli*, *P. aeruginosa* and *A. fumigates* and significant for *B. subtilis* and *C. albicans*. Cd(II) showed very highly significant against *E. coli* and *S.*

aureus. The U(VI) showed highly significant against *S. aureus* and *P. aeruginosa* and significant difference for *B. subtilis* and *A. fumigates*.

Such increased activity of metal chelate can be explained on the basis of the oxidation state of the metal ion, overtone concept and chelation theory. According to the overtone concept of cell permeability, the lipid membrane that surrounds the cell favors the passage of only lipid-soluble materials in which liposolubility is an important factor that

controls the antimicrobial activity. On chelation the polarity of the metal ion will be reduced to a greater extent due to overlap of ligand orbital and partial sharing of the positive charge of the metal ion with donor groups. Further it increases the delocalization of π -electrons over the whole chelate ring and enhances the lipophilicity of the complexes^{17, 39-41}. This increased lipophilicity enhances the penetration of complexes into the lipid membranes and blocks the metal binding sites in enzymes of microorganisms. These complexes also disturb the respiration process of the cell and thus block the synthesis of proteins, which restricts further growth of the microorganisms.

REFERENCES

1. Goodman L, Gilman A. Goodman & Gilman's the Pharmacological Basis of Therapeutics, 11th Ed., Mc Graw-Hill, New York, 2006.
2. Lindholm L, Carlberg B, Samuelsson O. Should beta blockers remain first choice in the treatment of primary hypertension? A meta-analysis. *Lancet*, 2005, 366:1545-1553.
3. Guidelines Committee, 2003 ESH-ESC Guidelines for the Management of Arterial Hypertension. *J. Hypertension*, 2003, 21:1011-1053.
4. Gilman A, Goodman L. The Pharmacological Basics of Therapeutics, 7th Ed., Macmillan, New York, 1985, 202.
5. Mehvar R, Brocks DR. Stereospecific pharmacokinetics and pharmacodynamics of beta-adrenergic blockers in humans. *J. Pharm. Pharm. Sci.*, 2001; 4(2):185-200.
6. Esteves de Castro RA, Canotilho J, Barbosa RM, Redinha JS. Infrared spectroscopy of racemic and enantiomeric forms of atenolol. *Spectrochimica Acta Part A*, 2007; 67(5): 1194-1200.
7. R. Bhushan R, Tanwar S. Different approaches of impregnation for resolution of enantiomers of atenolol, propranolol and salbutamol using Cu(II)-l-amino acid complexes for ligand exchange on commercial thin layer chromatographic plates. *Chromatography A*, 2010; 1217(8):1395-1398.
8. Cozar O, Szabo L, Cozar I, Leopold N, David L, Cainap C, Chis V. Spectroscopic and DFT study of atenolol and metoprolol and their copper complexes. *Molecular Structure*, 2011, 993(1-3):357-366.
9. Pyramides G, Robinson J, William Zitot S. The combined use of DSC and TGA for the thermal analysis of atenolol tablets. *pharmaceutical & Biomedical Analysis*, 1995; 13(2):103-110.
10. Yousef TA, Abu El-Reassh GM, El-Gammal OA, Ahmed SF. Structural, DFT and biological studies on Cu(II) complexes of semi and thiosemicarbazide ligands derived from diketo hydrazide. *Polyhedron*, 2014; 81:749-763.
11. Beecher DJ, Wong AC. Identification of hemolysin BL-producing *B. cereus* by a discontinuous hemolytic pattern in blood agar. *Appl. Environ. Microbiol.*, 1994; 60:1646.
12. Fallik E, Klein J, Grinberg S, Lomaniee E, Lurie S, Lalazar A. Effect of postharvest heat treatment of tomatoes on fruit ripening and decay caused by *Botrytis cinerea*. *Plant Dis.*, 1993; 77:985-988.
13. Vogel AI. Qualitative Inorganic analysis, 6th Ed. Wiley, New York, 1987.
14. LÍgia Maria M. Vieira et al. Synthesis and antitubercular activity of palladium and platinum complexes with fluoroquinolones. *European Journal of Medicinal Chemistry*, 2009; 44(10): 4107-4111..
15. Jimenez-Garrido N, Perello L, Ortiz R, Alzuet G, Gonzalez-Alvarez M, Canton E, Liu-Gonzalez M, Garcia-Granda S, Perez-Priede MJ Antibacterial studies, DNA oxidative cleavage, and crystal structures of Cu(II) and Co(II) complexes with two quinolone family members, ciprofloxacin and enoxacin. *Inorg. Biochem.*, 2005; 99(3):677-689.
16. Sadeek SA, El-Attar MS, Abd El-Hamid SM Synthesis, characterization and antibacterial activity of some new transition metal complexes with ciprofloxacin-imine. *Bull. Chem. Soc. Ethiop.*, 2015; 29(2):259-274.
17. Hughes MN. The inorganic chemistry of biological processes, 2nd Ed., Wiley Interscience, New York, 1981.
18. Almodfa H, Said AA, Nour EM. Preparation and infrared and thermal studies of. [UO₂(salen)(DMF)]. *Bull. Soc. Chem. Fr.*, 1991, 128:137-139.
19. Sadeek SA, Teleb SM, Refat MS, Elmosallamy MAF. Preparation, thermal and vibrational studies of UO₂(acac-o-phdn)(L)(L=H₂O, py, DMF and Et₃N). *J. Coord. Chem.*, 2005; 58:1077-1085.
20. Silverstein RM, Bassler GC, Morrill TC. Spectroscopic Identification of Organic Compounds, 5th Ed., Wiley, New York, 1991.
21. Nakamoto K. Infrared Spectra of Inorganic and Coordination Compounds, Wiley, New York, 1963.
22. McGlynnm SP, Smith JK, Neely WC. Electronic structure, spectra, and magnetic properties of

- oxycations. III. Ligation effects on the infrared spectrum of the uranyl ion. *J. Chem. Phys.*, 1961, 35:105-106.
23. Jones LH. Determination of U–O bond distance in uranyl complexes from their infrared spectra. *Spectrochim. Acta*, 1959, 15:409-411.
24. Nour EM, AL-Kority AM, Sadeek SA, Teleb SM. Synthesis and spectroscopic of NN-Ophenylene bis (salicylideneiminato) dioxouranium (VI) solvates (L) (L=DMF and Py). *Synth. React. Inorg. Met-Org. Chem.*, 1993; 23:39-52.
25. Bandoli G, Clemente DA, Croatto U, Vidali M, Vigato PA. Preparation and crystal molecular structure of N'-o -phenylene-bis (salicylideneiminato) UO₂(EtOH)]. *Chem. Commun.*, 1971; 1330-1331.
26. Pasomas G, Tarushi A, Efthimiadou EK. Synthesis, characterization and DNA-binding of the mononuclear dioxouranium(VI) complex with ciprofloxacin. *Polyhedron*, 2008; 27(1):133-138.
27. Refat MS. Synthesis and characterization of norfloxacin-transition metal complexes (group 11, IB): Spectroscopic, thermal, kinetic measurements and biological activity. *Spectrochim. Acta.*, 2007; 68(5):1393-1405.
28. Sadeek SA, EL-Shwiniy WH. Metal complexes of the fourth generation quinolone antimicrobial drug gatifloxacin: Synthesis, structure and biological evaluation. *J. Mol. Struct.*, 2010; 977:243-253.
29. Cotton FA, Wilkinson G, Murillo CA, Bochmann M. *Advanced Inorganic Chemistry*, 6th Ed., Wiley, New York, 1999.
30. Sadeek SA, El-Attar MS, Abd El-Hamid SM. Complexes and chelates of some bivalent and trivalent metals with ciprofloxacin Schiff base. *Synth. React. Inorg. Met. Org. Chem.*, 2015, 45(9):1412–1426.
31. Skauge T, Turel I, Sletten E. Interaction between ciprofloxacin and DNA mediated by Mg²⁺ ions. *Inorg. Chem. Acta.*, 2002, 339:247.
32. Sadeek SA, EL-Shwiniy WH, Zordok WA, EL-Didamony AM. Spectroscopic, structure and antimicrobial activity of new Y(III) and Zr(IV)ciprofloxacin. *Spectrochim. Acta. Part A*, 2011; 78(2):854-867.
33. Brzyska W, Hakim M. Hippurates of Mn(II),Cd(II) and Ag(I). *Polish, J. Chem.*, 1992, 66:413-418.
34. Sadeek SA, Refat MS, Teleb SM, El-Megharbel SM. Synthesis and characterization of V(III), Cr(III) and Fe(III) hippurates. *J. Mol. struct.*, 2005; 737(2-3):139-145.
35. Coats AW, J.P. Redfern JP. Kinetic Parameters from Thermogravimetric Data. *Nature*, 1964; 201:68-69.
36. Horowitz HH, Metzger G. New analysis of thermogravimetric traces. *Anal. Chem.*, 1963; 35(10):1464-1468.
37. Mahmoud WH, Mohamed GG, El-Dessouky MMI. Coordination modes of bidentate lornoxicam drug with some transition metal ions. Synthesis, characterization and in vitro antimicrobial and antitumor activity studies. *Spectrochim. Acta Part A*, 2014;122:598-608.
38. El-Megharbel SM, Hamza RZ, Refat MS. Synthesis, chemical identification, antioxidant capacities and immunological evaluation studies of a novel silver(I) carbocysteine complex. *Chem. Biol. Interact.*, 2014, 220:169-180.
39. Muhammad I, Javed I, Shahid I, Nazia I. In vitro antibacterial studies of Ciprofloxacin-imines and their complexes with Cu(II), Ni(II), Co(II) and Zn(II). *Turk. J. Biol.*, 2007, 30:67-72.
40. Anacona JR, Toledo C. Synthesis and antibacterial activity of metal complexes of ciprofloxacin. *Trans. Met. Chem.*, 2001; 26(1):228-231.
41. Efthimiadou EK, Karaliota A, Pasomas G. Metal complexes of the third-generation quinolone antimicrobial drug sparfloxacin: Structure and biological evaluation. *J. Inorg. Biochem.*, 2010; 104(4):455-466.